LAWRENCE
LIVERMORE
NATIONAL
LABORATORY

LLNL-TR-510234

FY2011 Progress Report: Agreement 8697 - NOx Sensor Development

L. Y. Woo, R. S. Glass

November 2, 2011

Disclaimer

This work performed under the auspices of the U.S. Department of Energy by Lawrence Livermore National Laboratory under Contract DE-AC52-07NA27344.

Agreement 8697 - NO_x Sensor Development

Leta Y. Woo and Robert S. Glass
Lawrence Livermore National Laboratory
P.O. Box 808, L-103
Livermore, CA 94551-9900
(925) 423-7140; fax: (925) (422-5844); e-mail: glass3@llnl.gov

DOE Technology Manager: Jerry L. Gibbs
(202) 586-1182; fax: (202) 586-1600; e-mail: jerry.gibbs@ee.doe.gov

Contractor: Lawrence Livermore National Laboratory, Livermore, California
Prime Contract No.: W-7405-Eng-48; LLNL-TR-510234

Objectives

- Develop an inexpensive, rapid-response, high-sensitivity and selective electrochemical sensor for oxides of nitrogen (NO_x) for compression-ignition, direct-injection (CIDI) OBD II systems
- Explore and characterize novel, effective sensing methodologies based on impedance measurements and designs and manufacturing methods that are compatible with mass fabrication
- Collaborate with industry in order to (ultimately) transfer the technology to a supplier for commercialization

Approach

- Use an ionic (O^{2-}) conducting ceramic as a solid electrolyte and metal or metal-oxide electrodes
- Correlate NO_x concentration with changes in cell impedance
- Evaluate sensing mechanisms and aging effects on long-term performance using electrochemical techniques
- Collaborate with Ford Research Center to optimize sensor performance and perform dynamometer and on-vehicle testing

Accomplishments

- Completed licensing of the LLNL NO_x technology to a company, EmiSense Technologies, LLC, which is located in Salt Lake City and has extensive resources for the development of advanced emission technology
- Used dynamometer testing to demonstrate application of cross-sensitivity mitigation strategies and to confirm robust performance of LSM sensor prototype while also using additional advanced emission test protocols requested by commercialization entities
- Publications/Presentations:
  - L.Y. Woo, R.S. Glass, R.F. Novak, and J.H. Visser, "Diesel engine dynamometer testing of impedancemetric NO_x sensors." *Sensor Actuat. B-Chem.*, 157:115-121, 2011.
  - L.Y. Woo, R.S. Glass, R.F. Novak, and J.H. Visser, "Impedance Analysis of High-Temperature Electrochemical NO_x Sensor Based on Porous Yttria-Stabilized Zirconia (YSZ)," 2011 Spring Meeting of the Materials Research Society, San Francisco, California, April 25-29, 2011.
  - L.Y.Woo and R. S. Glass, "NO_x Sensor Development," project ID #PM005, Annual Merit Review and Peer Evaluation. Washington, D.C., June 10, 2010

Future Directions

- Continue developing more advanced prototypes suitable for cost-effective, mass manufacturing and for optimizing performance, including long-term stability and cross-sensitivity, in laboratory, dynamometer, and on-vehicle tests
- Develop CRADA with EmiSense Technologies, LLC and initiate collaborative program along with Ford Motor Company to bring the NO_x sensor technology to commercialization and mass production (project on-vehicles by 2016)

Introduction

NO_x compounds, specifically NO and NO_2, are pollutants and potent greenhouse gases. Compact and inexpensive NO_x sensors are necessary in the next generation of diesel (CIDI) automobiles to meet government emission requirements and enable the more rapid introduction of more efficient, higher fuel economy CIDI vehicles.[1-3]

Because the need for a NO_x sensor is recent and the performance requirements are extremely challenging, most are still in the development phase.[4-6] Currently, there is only one type of NO_x sensor that is sold commercially, and it seems unlikely to be able to meet more stringent future emission requirements.

Automotive exhaust sensor development has focused on solid-state electrochemical technology, which has proven to be robust for in-situ operation in harsh, high-temperature environments (e.g., the oxygen stoichiometric sensor). Solid-state sensors typically rely on yttria-stabilized zirconia (YSZ) as the oxygen-ion conducting electrolyte, which has been extensively explored, and then target different types of metal or metal-oxide electrodes to optimize the response.[2-6]

Electrochemical sensors can be operated in different modes, including amperometric (current based) and potentiometric (potential based), both of which are direct current (dc) measurements. Amperometric operation is costly due to the electronics necessary to measure the small sensor signal (nanoampere current at ppm NO_x levels), and cannot be easily improved to meet the future technical performance requirements. Potentiometric operation has not demonstrated enough promise in meeting long-term stability requirements, where the voltage signal drift is thought to be due to aging effects associated with electrically driven changes, both morphological and compositional, in the sensor.[7]

Our approach involves impedancemetric operation, which uses alternating current (ac) measurements at a specified frequency. The approach is described in detail in previous reports and several publications.[8-12] Impedancemetric operation has shown the potential to overcome the drawbacks of other approaches, including higher sensitivity towards NO_x, better long-term stability, potential for subtracting out background interferences, total NO_x measurement, and lower cost materials and operation.[8-11]

Past LLNL research and development efforts have focused on characterizing different sensor materials and understanding complex sensing mechanisms.[8-12] Continued effort has led to improved prototypes with better performance, including increased sensitivity (to less than 5 ppm) and long-term stability, with more appropriate designs for mass fabrication, including incorporation of an alumina substrate with an imbedded heater and a protective sensor housing (see Fig. 1). Using multiple frequency measurements, an algorithm has been developed to subtract out that portion of the response due to interfering species.

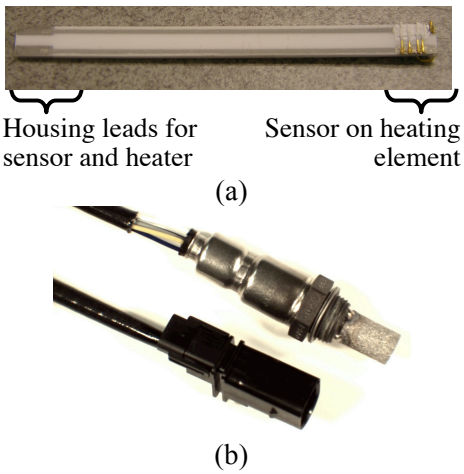

Figure 1. Picture of (a) alumina substrate with imbedded heater, provided by Ford Motor Company, suitable for packaging into (b) protective sensor housing.

Efforts in FY2011 have focused on using the previously developed algorithm to demonstrate how data from controlled laboratory evaluation could be applied to data from real-world engine testing. Other progress this year included dynamometer vehicle testing using advanced emission test protocols to confirm robustness and durability and also evaluating advanced material processing methods for mass manufacturing. As noted above, the LLNL NOx sensor technology has been licensed to EmiSense Technologies, located in Salt Lake City. This will greatly accelerate the commercialization for this technology.

Background

For a two-electrode electrochemical cell, impedancemetric sensing requires that at least one of the electrodes act as the "sensing" electrode with selective response to NO_x over other gas phase components. This contrasts to the case in potentiometric sensing, which relies on differential measurements between the two electrodes. The impedancemetric sensor design is quite flexible and can either contain one sensing electrode and one counter (i.e., non-sensing) electrode, or two sensing electrodes. It opens up the opportunity to use a wide variety of materials, both metal and metal oxides.

Both electrode composition and microstructure influence sensitivity, which relies on limiting the oxygen reaction on the electrode so that the NO_x reaction can be resolved.[9-11] In general, for the "sensing" electrode a dense microstructure is required with appropriate composition to limit the catalytic activity towards oxygen.[10-11]

Measured sensor impedance is a complex quantity with both magnitude and phase angle information. The phase angle has been found to provide a more stable response at higher operating frequencies and we prefer it for the sensor signal.[8-12]

In previous work, impedancemetric sensing using either gold or strontium-doped lanthanum manganite (LSM) electrodes, the latter being an electronically conducting metal oxide, was investigated in laboratory and engine testing. Preliminary results indicated that gold electrodes have good stability and the potential for low water cross-sensitivity, but also have a higher thermal expansion coefficient and lower melting temperature than the YSZ electrolyte, which limit processing flexibility. LSM electrodes have high melting temperatures and better thermal expansion match with YSZ, but have shown higher water cross-sensitivity than gold.

Experimental

The prototype incorporated a Au wire sensing electrode and a Pt counter electrode.[12] The prototype used a dense alumina substrate (99.6% Al_2O_3, 10 mm x 10 mm x 0.5 mm, Valley Design Corp.). The counter electrode was formed using platinum ink (Engelhard 6082) that was applied to the substrate and fired for two hours at 1200°C. A slurry of yttria-stabilized zirconia (YSZ) powder (Tosoh Corp., 8 mol% Y_2O_3-doped ZrO_2) mixed with ethanol, binder (polyvinyl butyral, Butvar), dispersant (phosphate ester), and plasticizer (dipropylene glycol dibenzoate) was then applied on top of the fired Pt counter electrode. Au wire (0.25 mm diameter, Alfa Aesar) electrodes were wrapped around the entire substrate with additional YSZ slurry applied on top of the wires. The assembled prototype was fired for two hours at 1000°C. Figure 2 shows a schematic of the Au wire NO_x sensor prototype, which consists of porous Pt, porous YSZ, and dense Au wire. Additional ceramic adhesive (Ultra-Temp 516, Aremco Products, Inc.) was applied along the edges to secure the Au wire electrodes to the alumina substrate.

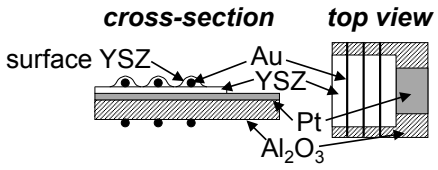

Figure 2. Schematic of Au wire NO_x sensor prototype.

Laboratory experiments were performed in a quartz tube (21.4 mm I.D.) placed inside a tube furnace with both electrodes exposed to the same environment. The gas composition was controlled by mixing air, N_2, and a 1000 ppm NO/NO_2 feed using a standard gas handling system equipped with thermal mass flow controllers. The total gas flow rate was fixed at 500 ml/min. The water concentration was controlled to approximately 2% by flowing mixtures of air and N_2 through a water bubbler and combining with dry mixtures of N_2, NO, and NO_2, which prevented NO_x from dissolving in the water. Measurements were made at 650°C.

Impedance measurements were performed using a Solartron 1260 Impedance Analyzer in combination with a Solartron 1287 Electrochemical Inter-

face, while engine testing at Ford used a stand-alone Solartron 1260 Impedance Analyzer. Computer-controlled data acquisition used the commercially available ZPlot software (Scribner Associates, Inc.).

Dynamometer testing of diesel engine exhaust was performed at Ford Research Center using an engine test cell with engine gas recirculation (EGR) and a urea-based selective catalytic reduction (SCR) system for reducing NO_x emissions. A portion of the tailpipe exhaust was extracted from the main exhaust and fed into a furnace containing the Au wire NO_x prototype sensor. Due to variations in the exhaust gas flow rate for different engine conditions, temperature fluctuations in the furnace were monitored using a thermocouple placed in close proximity to the sensor prototype. Measured temperatures ranged from approximately 650 to 670°C. A commercial NO_x sensor was located downstream of the prototype.

Data in tailpipe exhaust were obtained using a constant engine speed of 2750 rpm, and the exhaust gas composition was altered as described by the following. The exhaust gas composition, consisting of CH_4, NO, NO_2, NH_3, CO, CO_2, and H_2O, was determined using Fourier transform infrared (FTIR) spectroscopy, and O_2 concentration was determined using a paramagnetic oxygen analyzer.

A flow diagram of the dynamometer test setup is shown in Fig. 3. Two different protocols were used for the engine test. The first protocol involved constant throttle operation while stepping through different rates of urea injection, while the second protocol involved a fixed amount of urea injection while stepping through different percents of engine throttle.

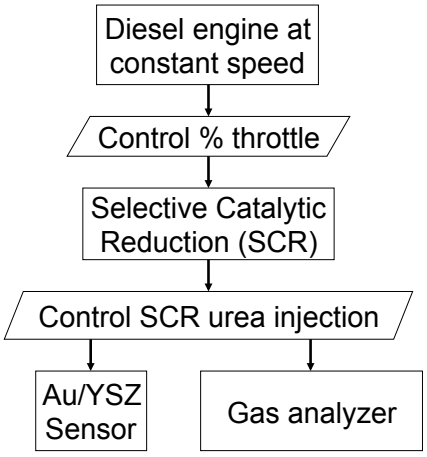

Figure 3. Simplified flow diagram of dynamometer test.

Results and Discussion

Laboratory testing of Au wire prototypes

Before testing in diesel engine dynamometer exhaust, laboratory testing of the Au wire NO_x prototype was conducted with controlled gas compositions. Figure 4a shows sensing behavior of the prototype using the phase angle as the measured response parameter, in degrees, at 10 Hz and 25 mV excitation as the input signal. Data were taken at 650°C in 10.5% O_2 and ~2% H_2O. The NO concentration was then adjusted in two-minute steps starting at a 0 ppm NO baseline. The NO concentration was then stepped to 100, 50, and 20 ppm, and at this point stepped in 5 ppm increments to 0 ppm and then back to 20 ppm, and then stepped to 50 and 100 ppm before returning to baseline. All changes, including the 5 ppm increments, are clearly resolved.

Figure 4b shows the phase angle response vs. NO concentration corresponding to the data shown in Fig. 4a. In Fig. 4b, the phase angle behavior was approximated using two separate linear regimes, one at low NO concentrations (0 to 20 ppm), and another at high NO concentrations (50 to 100 ppm). The sensitivity at low NO concentrations, as indicated by the slope (m_{low}), is ~0.05 deg/ppm NO, while the sensitivity decreased at high NO concentrations (m_{high}) to ~0.03 deg/ppm NO.

To investigate the effect of O_2 interference, laboratory testing also included measuring the phase angle response of the sensor over a range of O_2 concentrations: 4, 7, 10.5, and 12.6%. The phase angle vs. O_2 concentration is similar to the behavior in Fig. 4b, and could also be approximated using two separate linear regimes, one at low O_2 concentrations (4 to 7%, m_{low} of ~2 deg/% O_2), and another at high O_2 concentrations (10.5 to 12.6%, m_{high} of ~0.7 deg/% O_2). While it is possible to correct for the O_2 interference using a dual-frequency approach (as discussed in Ref. 8), in this study we used the measured O_2 concentration, which is described by the following.

Engine testing of Au wire prototype: Isolating influence of NO_x

After laboratory testing, the same Au wire prototype sensor was then evaluated in an engine dynamometer test cell. Two different protocols, as described in the experimental section, were used which either allowed for the isolation of the effect of NO_x or for the effect of O_2 interference.

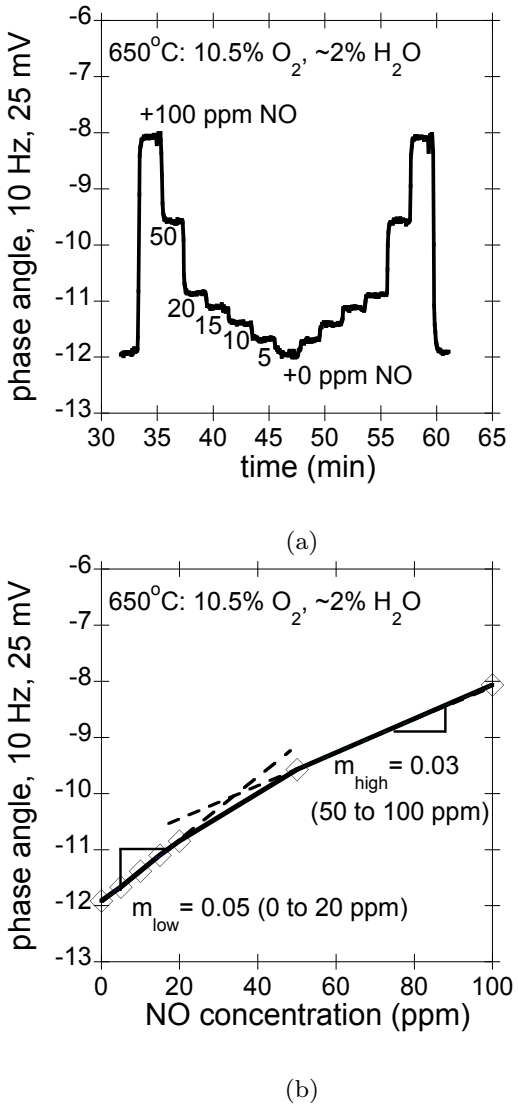

Figure 4. (a) Phase angle response of Au wire NO_x sensor prototype stepping in two min. increments through 0-100-50-20-15-10-5-0 ppm NO, and then reversing this sequence. (b) Corresponding plot of phase angle signal (deg) vs. NO concentration (ppm) with linear curve fits and calculated slopes (m_{low} and m_{high}).

To isolate the effect of NO_x, the engine was first operated under constant percent throttle and rate of urea injection until reaching minimal levels of NO_x. Then, the rate of urea injection was lowered in steps about every ten minutes, before finally being turned off. The results are shown in Fig. 5a, which includes a comparison of the prototype sensor response, results from gas analysis using Fourier transform infrared (FTIR) spectroscopy, and a commercial sensor signal (located downstream of the prototype).

In Fig. 5b, it is observed that the predominant NO_x species during engine testing was NO, with low levels of NO_2 and NH_3. The decreasing frequency of the urea injection levels led to smaller amounts of urea in the SCR to react with the NO_x, and therefore higher concentrations of NO in the exhaust. Measurements of O_2, CO_2, H_2O, CO, and CH_4 in the exhaust taken concurrently with the data shown in Fig. 5 show minimal changes and therefore cannot be used to explain changes seen in the measured sensor response. In addition, only small temperature changes were measured during this test, in the range of ~664 to ~670°C (see Fig. 5c), and showed no correlation with the measured response from the NO_x prototype, indicating that the measured response is fairly tolerant to changes in temperature over at least this range.

Specific requirements for the NO_x sensor will ultimately depend on the design of the entire exhaust after-treatment system, which is currently in development. However, the most promising technologies being investigated suggest that the sensor will need to detect levels typically less than ~20 ppm NO_x. As shown in Fig. 4b, laboratory testing has demonstrated that the NO_x prototype had better sensitivity at lower concentrations (less than 20 ppm) than at higher concentrations.

Figure 5a shows that both the commercial sensor and FTIR match over this concentration range. The prototype response qualitatively tracks the commercial sensor and FTIR measurements; however, the sensitivity differs, with more pronounced differences at NO concentrations higher than ~100 ppm. The behavior of the prototype sensor in engine testing appears to show higher sensitivity to NO at lower concentrations, which is in agreement with results from laboratory evaluation (Fig. 4b).

To account for the different sensitivities at high and low NO concentrations, an adjustment was applied to the measured phase angle (θ_{meas}) in engine dynamometer testing using the laboratory data. The adjusted values for the phase angle signal (θ_{adj}) were calculated using the two different sensitivity values shown in Fig. 4b. The adjusted values are given by the following equations:

$$\theta_{adj} = \theta_{baseline} + \Delta\theta_{adj} \quad (1)$$

$$\Delta\theta_{adj} = \frac{\theta_{meas} - \theta_{baseline}}{m_{high}} m_{low} \quad (2)$$

The measured phase angle at the initial prevalent NO_x concentration of ~30 ppm was used as the baseline ($\theta_{baseline}$), which was measured from about 80 to 86 min in Fig. 5 with a value of about -14 deg.

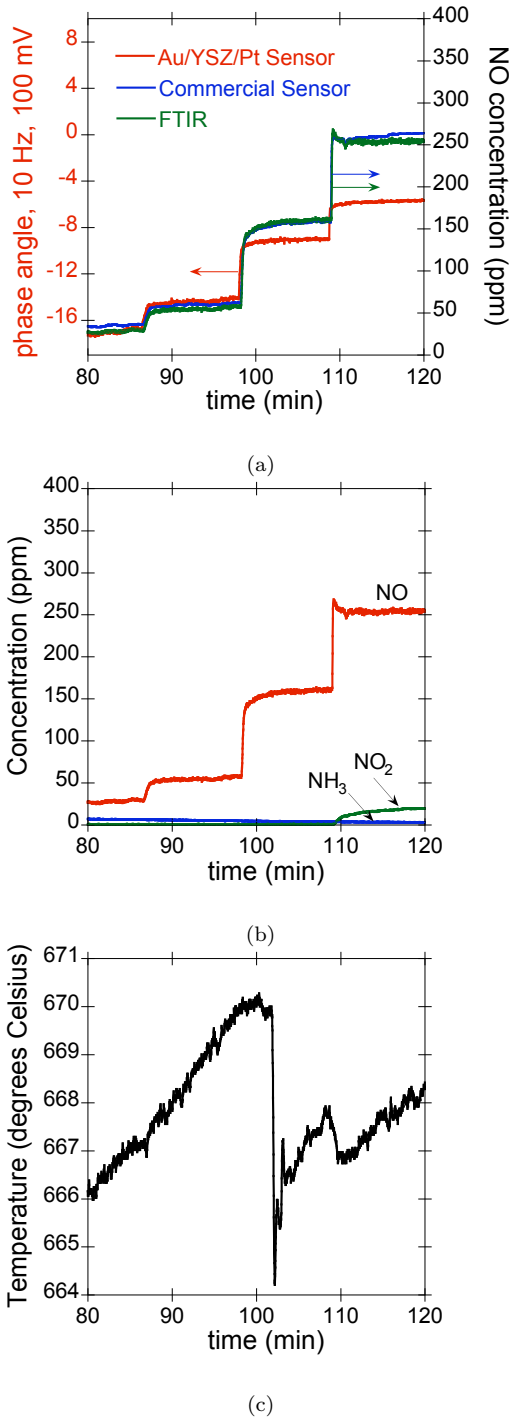

Figure 5. Dynamometer test: (a) Phase angle response of Au wire prototype sensor (red, left y-axis) compared with a commercial sensor (blue, right y-axis) and FTIR gas analysis (green, right y-axis); (b) FTIR results for NO, NO_2, and NH_3; and (c) variation in temperature.

Figure 6 shows the adjusted phase angle signal after accounting for the sensitivities at different NO concentrations, which has better agreement with both the commercial sensor and FTIR compared to the raw data shown in Fig. 5a.

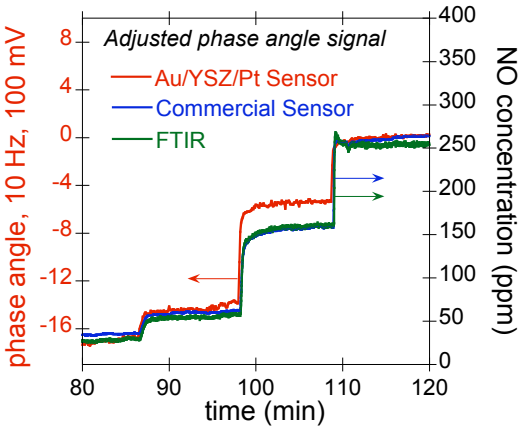

Figure 6. Adjusted phase angle response of Au wire prototype sensor (red, left y-axis) shows better agreement with a commercial sensor (blue, right y-axis) and FTIR (green, right y-axis) compared to raw data in Fig. 5a.

In Fig. 6, the adjusted sensor signal for ~150 ppm, measured from 100 to 110 min, shows less correlation between the prototype and the commercial sensor and FTIR measurements, indicating that the linear approximation extracted form from laboratory evaluation does not completely account for the nonlinear sensitivity over the entire range of concentrations of NO.

Engine testing of Au wire prototype: O_2 interference

The second protocol used investigated the effect of O_2 cross-sensitivity where the engine was again first operated under constant percent throttle and rate of urea injection with low levels of NO_x. The level of urea injection was then kept constant while the percent throttle was first increased and then stepped to lower levels. The results are shown in Fig. 7a, including a comparison of the prototype sensor with FTIR results and the commercial sensor signal. As shown in Fig. 7b, the predominant NO_x species measured by FTIR was NO, with very low levels of NO_2 and NH_3. The initial increase in percent throttle at 19 min corresponded to an abrupt increase in the level of NO, with progressively decreasing amounts of NO at lower percent throttle.

Figure 8 shows measurements for O_2, CO_2, H_2O, CO, and CH_4 taken during the same engine testing

cycle shown in Fig. 7. The initial percent throttle increase corresponded to an increase in CO_2 and H_2O, and a decrease in O_2. Subsequent changes to lower percent throttle levels corresponded to decreasing amounts of CO_2 and H_2O, and increasing amount of O_2. The CO and CH_4 concentrations were in all cases low and constant during engine testing. Temperature variations did not show a correlation with sensor response, indicating that the measured signal is fairly tolerant to temperature changes over the measured range of ~654 to ~660°C.

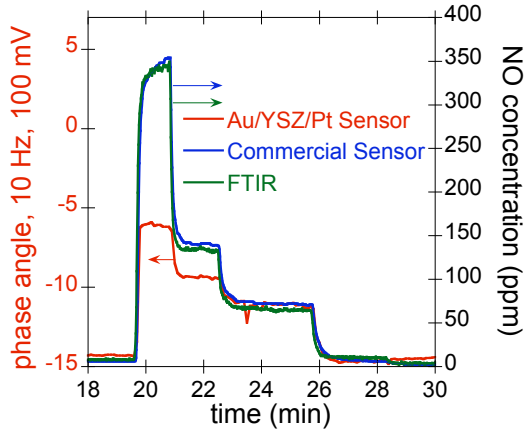

(a)

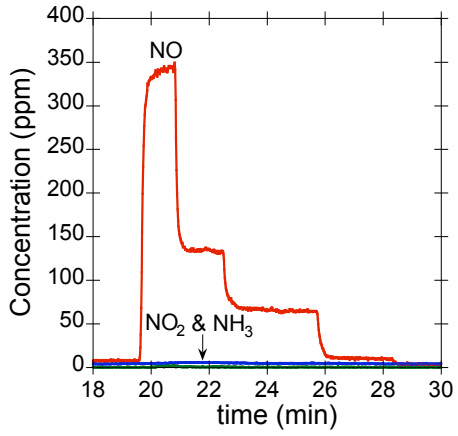

(b)

Figure 7. Dynamometer test with O_2 interference: (a) Phase angle response of Au wire prototype sensor (red, left y-axis) compared with a commercial sensor (blue, right y-axis) and FTIR gas analysis (green, right y-axis); (b) FTIR results for NO, NO_2, and NH_3.

In Fig. 8, both CO_2 and H_2O changed over a range of ~2%, while O_2 concentration changed over a range twice as large, from about 5 to 9%. Laboratory evaluation indicated that changes in O_2 from 4 to 7% corresponded to a phase angle sensitivity of about 2 deg/% O_2 (see discussion above). Therefore, changes in both O_2 and NO_x concentration influenced the measured phase angle signal.

To compensate for the O_2 interference in the measured phase angle (θ_{meas}), an adjustment was applied using the measured O_2 concentration, $[O_2]_{meas}$, and the sensitivity values for low O_2 concentrations (4 to 7%, m_{low} = 2 deg/% O_2). A baseline value for the measured O_2, $[O_2]_{baseline}$, was chosen at the initial concentration of ~9%, shown in Fig. 8. The adjusted values were calculated using the following equations:

$$\theta_{O2,adj} = \theta_{meas} - \Delta\theta_{O2} \quad (3)$$

$$\Delta\theta_{O2} = \left([O_2]_{meas} - [O_2]_{baseline}\right) m_{low} \quad (4)$$

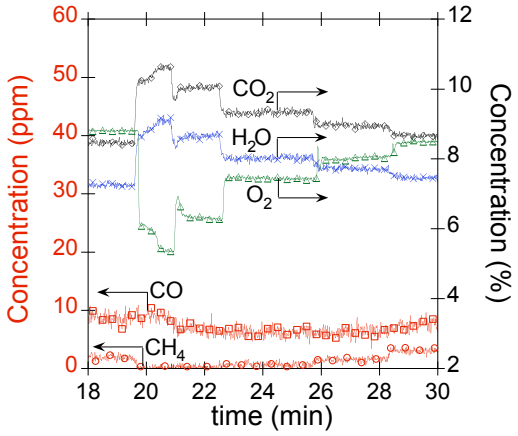

Figure 8. Dynamometer test with O_2 interference showing steady-state values for CO and CH_4 and changes in CO_2, H_2O, and O_2.

In addition to the O_2 interference adjustment (Eqs. 3 and 4), the different NO sensitivity at low and high concentrations also needed to be accounted for (Eqs. 1 and 2 as discussed above). Therefore, the phase angle adjusted for O_2 interference ($\theta_{O2,adj}$) was then used in Eqs. 1 and 2, where $\theta_{meas} = \theta_{O2,adj}$. The same sensitivity values were used as before, given by the two slopes in Fig. 4b, and an appropriate baseline value ($\theta_{baseline}$) was chosen.

Figure 9 shows the adjusted phase angle signal after accounting for both the O_2 interference and the different sensitivities at low and high NO concentrations.

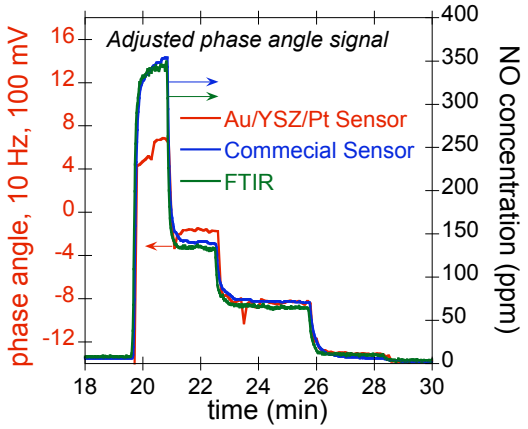

Figure 9. Adjusted phase angle response of Au wire prototype sensor (red, left y-axis), and commercial (blue, right y-axis) and FTIR (green, right y-axis).

The adjusted phase angle signal has better agreement with both the commercial sensor and FTIR. However, data at higher NO concentrations greater than ~100 ppm show less agreement, again indicating that the linear approximation from laboratory testing does not completely account for the nonlinear sensitivity over the entire range of concentrations. Furthermore, although changes in both CO_2 and H_2O occurred over a small 2% range, they could also be contributing to the measured phase angle signal.

Conclusions

Work in FY2011 focused on using an algorithm developed in FY2010 in a simplified strategy to demonstrate how data from controlled laboratory evaluation could be applied to data from real-world engine testing. The performance of a Au wire prototype sensor was evaluated in the laboratory with controlled gas compositions and in dynamometer testing with diesel exhaust. The laboratory evaluation indicated a nonlinear dependence of the NO_x and O_2 sensitivity with concentration. For both NO_x and O_2, the prototype sensor had higher sensitivity at concentrations less than ~20 ppm and ~7%, respectively, compared to lower NO_x and O_2 sensitivity at concentrations greater than ~50 ppm and ~10.5%, respectively. Results in dynamometer diesel exhaust generally agreed with the laboratory results. Diesel exhaust after-treatment systems will likely require detection levels less than ~20 ppm in order to meet emission regulations.

The relevant mathematical expressions for sensitivity in different concentration regimes obtained from bench-level laboratory evaluation were used to adjust the sensor signal in dynamometer testing. Both NO_x and O_2 exhibited non-linear responses over the concentration regimes examined (0-100 ppm for NO_x and 4-7% for O_2). Adjusted sensor signals had better agreement with both a commercial NO_x sensor and FTIR measurements. However, the lack of complete agreement indicated that it was not possible to completely account for the nonlinear sensor behavior in certain concentration regimes. The agreement at lower NO_x levels (less than 20 ppm) was better than at higher levels (50-100 ppm).

Other progress in FY2011 included dynamometer testing of sensors with imbedded heaters and protective housings that were mounted directly into the exhaust manifold. Advanced testing protocols were used to evaluate the sensors. These experiments confirmed the potential for sensor robustness and durability. Advanced material processing methods appropriate for mass manufacturing, such as sputtering, are also being evaluated. A major milestone for this past year was the licensing of the LLNL NO_x sensor technology to EmiSense Technologies, LLC. EmiSense has extensive experience and resources for the development of emission control sensors. A CRADA is in development that will allow LLNL to work in partnership with EmiSense to bring the LLNL NO_x sensor technology to commercialization. Ford Motor Company is also a partner in this effort.

References

1. N. Yamazoe, *Sens. Actuators, B*, **108**, 2 (2005).
2. R. Moos, *Int. J. Appl. Ceram. Technol.*, **2**, 401 (2005).
3. S. Akbar, P. Dutta, and C. Lee, *Int. J. Appl. Ceram. Technol.*, **3**, 302 (2006).
4. F. Menil, V. Coillard, and C. Lucat, *Sensors and Actuators B,* **67**, 1 (2000).
5. S. Zhuiykov and N. Miura, *Sens. Actuators, B*, **121**, 639 (2007).
6. J. W. Fergus, *Sens. Actuators, B*, **121**, 652 (2007).
7. S. -W. Song, L. P. Martin, R. S. Glass, E. P. Murray, J. H. Visser, R. E. Soltis, R. F. Novak, and D. J. Kubinski, *J. Electrochem. Soc.*, **153**, H171 (2006).

8. L. P. Martin, L. Y. Woo, and R. S. Glass, *J. Electrochem. Soc.,* **154**, J97 (2007).
9. L. Y. Woo, L. P. Martin, R. S. Glass, and R. J. Gorte *J. Electrochem. Soc.,* **154**, J129 (2007).
10. L. Y. Woo, L. P. Martin, R. S. Glass, W. Wang, S. Jung, R. J. Gorte, E. P. Murray, R. F. Novak, and J. H. Visser. *J. Electrochem. Soc.,* **155**, J32 (2008).
11. L.Y. Woo, R.S. Glass, R.F. Novak, and J.H. Visser. *J. Electrochem. Soc.*, **157**, J81 (2010).
12. L.Y. Woo, R.S. Glass, R.F. Novak, and J.H. Visser. *Sensor Actuat. B-Chem.*, **157**, 115 (2011).

Publications/Presentations

L.Y. Woo, R.S. Glass, R.F. Novak, and J.H. Visser. "Diesel engine dynamometer testing of impedancemetric NO_x sensors." *Sensor Actuat. B-Chem.*, 157:115-121, 2011.

L.Y. Woo, R.S. Glass, R.F. Novak, and J.H. Visser, "Impedance Analysis of High-Temperature Electrochemical NOx Sensor Based on Porous Yttria- Stabilized Zirconia (YSZ)," 2011 Spring Meeting of the Materials Research Society, San Francisco, California, April 25-29, 2011.

L.Y.Woo and R. S. Glass, "NOx Sensor Development," project ID #PM005, Annual Merit Review and Peer Evaluation. Washington, D.C., June 10, 2010.